Turbulent wake solutions of the Prandtl α equations

Vakhtang Putkaradze
Department of Mathematics and Statistics, University of New Mexico, Albuquerque, New Mexico 87131-1141

Patrick Weidman
Department of Mechanical Engineering, University of Colorado at Boulder, Boulder, Colorado 80309-0427

(Received 16 May 2002; published 25 March 2003)

A derivation of the Navier-Stokes α equations for spatially dependent α is presented. It is shown that an extra term in the equation is necessary to ensure the conservation of momentum. The Prandtl form of these variable α equations are determined for both planar and axisymmetric pressure-gradient-driven boundary-layer flows correcting previous work on the subject. The Prandtl equations are then solved analytically for four different asymptotic wake flows: the classical planar wake, the classical axisymmetric wake, the planar dragless wake, and the axisymmetric dragless wake. Least-squares fits of the theoretical solutions with available turbulent mean-flow velocity data for classical planar and axisymmetric wakes are given. We point out that the dissipation coefficient does not have to be equal to the kinematic viscosity, and its numerical value may be estimated from experimental data.

DOI: 10.1103/PhysRevE.67.036304 PACS number(s): 47.27.Eq, 47.27.Jv

I. INTRODUCTION

The Lagrangian averaged Navier-Stokes α (NS-α) equations were recently proposed [1] as a model for averaged velocity fields in turbulent flow. These equations have the following form: if $\mathbf{u}(\mathbf{x},t)$ is the *averaged* velocity of the turbulent flow, and α is a constant representating the rms (root mean square) of Lagrangian fluctuations, then $\mathbf{u}(\mathbf{x},t)$ satisfies

$$\frac{\partial \mathbf{v}}{\partial t}+(\mathbf{u}\cdot\boldsymbol{\nabla})\mathbf{v}+v_j\boldsymbol{\nabla}u_j+\boldsymbol{\nabla}Q=\Lambda\Delta\mathbf{v}, \tag{1a}$$

$$\boldsymbol{\nabla}\cdot\mathbf{u}=0, \tag{1b}$$

$$\mathbf{v}=\mathbf{u}-\alpha^2\Delta\mathbf{u}, \tag{1c}$$

where Λ plays the role of viscosity and Eq. (1c) connects momentum $\mathbf{v}$ and velocity $\mathbf{u}$ through the Helmholtz operator. In previous work on the subject, the constant Λ was taken to be equal to the kinematic viscosity of the fluid ν so that Eq. (1) reduces to the Navier-Stokes equation as $\alpha\to 0$. This formulation is mathematically interesting, since the existence and uniqueness of solutions have been established for Eq. (1) in three dimensions [2,3], whereas the same results for the Navier-Stokes equations are missing. From the practical point of view, system (1) permits modeling of turbulent flows whose best fit is determined by the choice of α. The derivation of the Euler α equations [i.e., system (1) with $\Lambda=0$] is rigorous, but the introduction of the viscous term on the right-hand side of Eq. (1a) is *ad hoc*. In particular, we believe that the constant Λ in front of the dissipation term does not have to be equal to kinematic viscosity, as the limit of $\alpha\to 0$ is not physical. Indeed, $\alpha\to 0$ corresponds to the flow becoming laminar, since α is the rms of Lagrangian fluctuation of the trajectory. The coefficients Λ and α therefore are dependent on the flow parameters (in particular, on the suitably defined Reynolds number) and must be fitted to experimental data. We also note that even though authors in Ref. [1] achieved excellent fit to experimental data in channels and pipes for $\Lambda=\nu$, the analytical expression for their fitting curves will remain the same in the case when Λ is arbitrary, since for pipe and channel flows the solutions of Eq. (1) are given by $\Delta\mathbf{v}=$const. Therefore, an ongoing effort is under way to derive a variety of test cases using this model for comparison with available experimental data. Turbulent boundary-layer flows are ideal for this task, since in the equations for these flows (Prandtl α equations, see below), we can scale out the value of Λ and fit the shape of velocity profile using only one parameter (a rescaled α). The dissipation coefficient Λ affects only the thickness of the flow and can be deduced from experimental data independently. Hence, only a one-parameter fit to experimental data is required.

In the current study, we determine the asymptotic form of mean turbulent wake profiles described by the Prandtl limit of the NS-α equations in both two and three dimensions, with equal consideration given to classical wakes and to momentumless wakes behind self-propelled bodies.

In Sec. II, a derivation of the generalized NS-α equations, valid for spatially varying α, is outlined. In Sec. III, the thin-layer approximation to the generalized NS-α equations, herein referred to as the Prandtl α equations, is developed for both planar and axisymmetric boundary-layer flows. With the exception of stagnation-point flows and a couple of other simple flow configurations, the cross-stream thickness of a turbulent boundary layer varies (increases) with the streamwise direction, taken here to be x, in which case it is entirely probable that α will vary with x.

Recently, a form of the Prandtl α boundary-layer equations was reported by Cheskidov [4]. Unfortunately, we have found Cheskidov's equations to be incorrect owing to their failure to conserve streamwise momentum flux. Indeed, it was this inconsistency that motivated our reconsideration of the results in Ref. [1] to seek a more general form of the NS-α equations valid for streamwise varying α. We discuss the physical and mathematical differences between our and

Cheskidov's version of the Prandtl α equations at the end of Sec. III.

Application of the generalized NS-α equations to mean turbulent wake flows, both classical and momentum-free, are presented in Secs. IV and V. To leading order, the spatial dependence of α does not enter into the analysis because the weak velocity defect in the far wake permits a linearization of the advection terms. However, further corrections to the asymptotic solutions would include a contribution from the variability of α.

II. THE NAVIER-STOKES α EQUATIONS FOR VARIABLE α

For clarity, we begin our formulation of the generalized NS-α equations for variable α with a brief derivation of the Euler α equations obtained through application of variational methods as given in Ref. [1]. Lagrangian coordinates $\mathbf{X}(\mathbf{a},t)$ denote the position of a fluid particle at time t originating at point $\mathbf{a}$. The kinetic energy is given by $\int d^3\mathbf{a}\dot{\mathbf{X}}^2$. Fluid incompressibility is enforced by the requirement

$$D \equiv \det\left(\frac{\partial \mathbf{X}}{\partial \mathbf{a}}\right) = 1. \tag{2}$$

Introduction of a Lagrange multiplier q to account for Eq. (2) leads to the energy functional

$$\mathcal{L} = \int d^3\mathbf{a}\left[\dot{\mathbf{X}}^2 + q\left\{1 - \det\left(\frac{\partial \mathbf{X}}{\partial \mathbf{a}}\right)\right\}\right]. \tag{3}$$

Taking the variation of $\mathcal{L}$ with respect to $\mathbf{X}$ and using the relation $\ln(\det \mathcal{M}) = \mathrm{tr}(\ln \mathcal{M})$ for square matrix $\mathcal{M}$, we arrive at the Euler equations in Lagrangian coordinates

$$\ddot{\mathbf{X}} - \boldsymbol{\nabla} q = \mathbf{0}. \tag{4}$$

In Eulerian coordinates, $\dot{\mathbf{X}} = \hat{\mathbf{u}}$ and $\ddot{\mathbf{X}} = \hat{\mathbf{u}}_t + (\hat{\mathbf{u}}\cdot\boldsymbol{\nabla})\hat{\mathbf{u}}$, Eq. (4) reduces to the familiar form of Euler equations in Eulerian coordinates, in which q plays the role of the thermodynamic pressure. Here $\hat{\mathbf{u}}$ is the instantaneous particle velocity, not to be confused with $\mathbf{u}$ which is the averaged turbulent flow velocity.

Let us now consider a more general Lagrangian which depends on the spatial coordinates

$$\mathcal{L} = \int d^3\mathbf{a}\left[F(\dot{\mathbf{X}},\mathbf{X}) + q\left\{1 - \det\left(\frac{\partial \mathbf{X}}{\partial \mathbf{a}}\right)\right\}\right]. \tag{5}$$

Here F is an arbitrary function of $\mathbf{X}$ and $\dot{\mathbf{X}}$ and in this case, the Euler equations are

$$\frac{d}{dt}\frac{\partial F}{\partial \dot{\mathbf{X}}} - \frac{\partial F}{\partial \mathbf{X}} - \boldsymbol{\nabla} q = 0. \tag{6}$$

Now in Eulerian coordinates, the variational equation for the velocity $\mathbf{u} = \dot{\mathbf{X}}$ is

$$\left(\frac{\partial}{\partial t} + \mathbf{u}\cdot\boldsymbol{\nabla}\right)\frac{1}{D}\frac{\delta \mathcal{L}}{\delta \mathbf{u}} + \frac{1}{D}\frac{\delta \mathcal{L}}{\delta u_j}\boldsymbol{\nabla} u_j + \frac{1}{D}\frac{\partial F}{\partial \mathbf{X}} - \boldsymbol{\nabla}\frac{\delta \mathcal{L}}{\delta D} = 0. \tag{7}$$

The Euler-Poincaré equations are identical to those obtained by Chen *et al.* [1] but with the additional term $1/D\,\partial F/\partial \mathbf{X}$ arising from the explicit spatial dependence of the Lagrangian. For analysis of average velocities in turbulent flows, we employ the Lagrangian introduced in Ref. [1], viz.,

$$\mathcal{L} = \int d^3\mathbf{X}\left\{\frac{D}{2}[|\mathbf{u}|^2 + \alpha^2|\boldsymbol{\nabla}\mathbf{u}|^2] + q[\langle \det(I + \boldsymbol{\xi}_{\mathbf{X}})\rangle - D] + (\langle \boldsymbol{\xi} \det(I + \boldsymbol{\xi}_{\mathbf{X}})\rangle \cdot \boldsymbol{\nabla})q\right\}, \tag{8}$$

where D is given by Eq. (2), q is the Lagrange multiplier for the incompressibility condition $D - 1 = 0$, $\boldsymbol{\xi}$ is the fluctuation of Lagrangian position, and $\langle \cdots \rangle$ is the ensemble average of fluctuations. As usual, it is assumed that $\langle \xi_i \xi_j \rangle = \delta_{ij}\alpha^2$. Taking the variation of the averaged Lagrangian (8) furnishes the generalized Euler α equations

$$\left(\frac{\partial}{\partial t} + \mathbf{u}\cdot\boldsymbol{\nabla}\right)\mathbf{v} + v_j\boldsymbol{\nabla} u_j + \frac{1}{2}(\boldsymbol{\nabla}\alpha^2)|\boldsymbol{\nabla}\mathbf{u}|^2 + \boldsymbol{\nabla} Q = 0, \tag{9a}$$

$$\boldsymbol{\nabla}\cdot\mathbf{u} = 0, \tag{9b}$$

$$\mathbf{v} = \mathbf{u} - \boldsymbol{\nabla}\cdot(\alpha^2\boldsymbol{\nabla}\mathbf{u}). \tag{9c}$$

Performing the spatial integration shows that Eq. (9a) indeed conserves momentum flux. More detailed derivation of Eq. (9a) is given in Ref. [5]. The final step is to add the momentum diffusion term to the right-hand side of Eq. (9a) to obtain the generalized NS-α equations

$$\left(\frac{\partial}{\partial t} + \mathbf{u}\cdot\boldsymbol{\nabla}\right)\mathbf{v} + v_j\boldsymbol{\nabla} u_j + \frac{1}{2}(\boldsymbol{\nabla}\alpha^2)|\boldsymbol{\nabla}\mathbf{u}|^2 + \boldsymbol{\nabla} Q = \Lambda\Delta\mathbf{v} \tag{10}$$

valid for spatially dependent α. Equations (9b) and (9c) are unchanged.

III. THE TWO-DIMENSIONAL PRANDTL α EQUATIONS

The Prandtl limit of the generalized NS-α equations in two dimensions are now obtained. As usual, we choose (x,y) as streamwise and cross-stream coordinates, respectively, with corresponding velocities (u_x,u_y). If the typical length scale is L_* and the typical velocity is U_*, the standard boundary-layer scalings $x = L_* X$, $y = \epsilon L_* Y$, $u_x = U_* U_x$, and $u_y = \epsilon U_y$, where $\epsilon \ll 1$ is the boundary-layer slenderness parmeter. Assuming $\alpha = \alpha(x)$ only, the scaling $\alpha(x) \to \epsilon L_* \alpha(X)$ is employed; note that lower case α is retained as the *scaled* variable for notational simplicity. Balancing the leading-order viscous term with the leading-order inertia terms in the x component of Eq. (9a) yields $\epsilon = \sqrt{\Lambda/(L_* U_*)}$. Thus, the thickness of boundary layer is proportional to $R_\Lambda^{-1/2}$, where R_Λ is the Reynolds number based on Λ. For laminar boundary layer, δ is proportional to

$R_\nu^{-1/2}$, where $R_\nu = LU_*/\nu$. This clearly shows that the effective viscosity Λ cannot be equal to the kinematic viscosity ν, since experiments [6] show that for turbulent boundary layers, $\epsilon \gg R_\nu^{-1/2}$. Now with all scales fixed, the streamwise and cross-stream components of Eq. (9a) are, respectively,

$$U_x \frac{\partial V_x}{\partial X} + U_y \frac{\partial V_x}{\partial Y} + V_x \frac{\partial U_x}{\partial X} + \frac{1}{2} \frac{\partial \alpha^2}{\partial X} \left(\frac{\partial U_x}{\partial Y} \right)^2 = -\frac{\partial Q}{\partial X} + \frac{\partial^2 V_x}{\partial Y^2}, \tag{11a}$$

$$V_x \frac{\partial U_x}{\partial Y} = -\frac{\partial Q}{\partial Y}. \tag{11b}$$

A term due to the spatial variation of α like that appearing in Eq. (11a) does not appear in Eq. (11b) since we have assumed $\alpha = \alpha(X)$ only. Finally, the streamwise momentum density V_x that appears in system (11) is, according to Eq. (9c), precisely

$$V_x = U_x - \left[\frac{\partial}{\partial X} \left(\epsilon^2 \alpha^2 \frac{\partial U_x}{\partial X} \right) + \alpha^2 \frac{\partial^2 U_x}{\partial Y^2} \right], \tag{12}$$

showing that the first term in the brackets may be neglected compared to the second in the boundary-layer formulation. Taking this into account, integration of Eq. (11b) on Y gives

$$Q(X,Y) = P(X) - \frac{1}{2} U_x^2 + \frac{\alpha^2}{2} \left(\frac{\partial U_x}{\partial Y} \right)^2. \tag{13}$$

Substitution of this expression into Eq. (11a) yields the Prandtl α system,

$$U_x \frac{\partial V_x}{\partial X} + U_y \frac{\partial V_x}{\partial Y} + \alpha^2 \left(\frac{\partial U_x}{\partial X} \frac{\partial U_x}{\partial Y} - \frac{\partial U_x}{\partial Y^2} \frac{\partial U_x}{\partial X} \right) + \frac{\partial \alpha^2}{\partial X} \left(\frac{\partial U_x}{\partial Y} \right)^2 = -\frac{dP}{dX} + \frac{\partial^2 V_x}{\partial Y^2}, \tag{14a}$$

$$\frac{\partial U_x}{\partial X} + \frac{\partial U_y}{\partial Y} = 0, \tag{14b}$$

$$V_x = U_x - \alpha^2 \frac{\partial^2 U_x}{\partial Y^2}. \tag{14c}$$

We emphasize that our version of the Prandtl α equations conserves momentum in the following sense. Integrating Eq. (14a) across a fluid domain $[Y_1, Y_2]$ yields

$$\frac{d}{dX} \int U_x V_x \, dY = \left. \frac{\partial V_x}{\partial y} \right|_{Y_1}^{Y_2}. \tag{15}$$

Since $\int U_x V_x \, dY$ is the total streamwise momentum flux, dissipation of momentum enters only through boundary ($Y_{1,2}$ finite) or far-field ($Y_{1,2} \to \infty$) effects; there are no bulk terms responsible for the change. The conservation of momentum flux is afforded by the coefficient in front of the last term on the left-hand side of Eq. (14a) being equal to 1, and not 1/2 as would be obtained from a straightforward application of boundary-layer scaling to the NS-α equations for constant α, as was done by Cheskidov [4] in the context of Blasius flow along a flat plate. Cheskidov's version of the Prandtl α equations fails to conserve streamwise momentum in the sense of Eq. (15). Since conservation laws play a major role in our discussion of wakes in Secs. IV and V and are also of crucial importance in the study of turbulent jets [7], having an equation yielding the conservation of momentum is essential.

Another interesting feature of Eq. (14a) is that the coefficient in front of viscous term is unity, and α remains the sole unknown parameter in the equation. Therefore, the velocity profiles can be fitted using one parameter only, and Λ can be found later by using the experimental data for the width of the flow, as is illustrated at the end of Sec. IV. We also note that the boundary-layer scaling in Ref. [4] was done for $\Lambda = \nu$ and therefore does not yield correct the thickness of the turbulent boundary layer.

IV. PLANAR WAKES

For application to planar wakes, we adopt the following simplified notation for variables in the generalized Prandlt α system (14). Mean velocities $(U_x, U_y) \Rightarrow (u, v)$, Helmholtzian velocities $(V_x, V_y) \Rightarrow (u_1, v_1)$, Cartesian coordinates $(X, Y) \Rightarrow (x, y)$, and $U_\infty = 1$ is the uniform stream far above, below and upstream of the symmetric planar body forming the wake. In lieu of the streamwise velocity u, we work with the deficit velocity $w = 1 - u$ which, for asymptotic far-field wakes, is small as compared to the freestream velocity. Thus, the dependent variables used for analyzing both the planar classical wake in Sec. IV A and the planar dragless wake in Sec. IV B are the wake deficit velocity

$$w = 1 - u \tag{16a}$$

and the Helmholtzian wake deficit velocity

$$w_1 = w - \alpha^2 w_{yy}, \tag{16b}$$

in which $\alpha = \alpha(x)$.

A. The classical wake

Inserting Eqs. (16) into the generalized Prandtl α equations (14) and linearizing yields the diffusion equation

$$\frac{\partial w_1}{\partial x} = \frac{\partial^2 w_1}{\partial y^2}. \tag{17}$$

Positing the similarity ansatz

$$w_1(x,y) = x^a F(\eta), \quad \eta = \frac{y}{x^b}$$

from Eq. (17), we find that $b=1/2$ so that the width of the wake grows proportionally to $\sqrt{x}$, which is consistent with experiments. That, in turn, gives the ordinary differential equation

$$F''=aF-\frac{1}{2}\eta F'. \tag{18}$$

To determine the constant a, we need to use the physical condition that momentum deficit in the wake is equal to the drag on the body responsible for the wake, viz.,

$$D\equiv\int_{-\infty}^{\infty}w_1\,dy=x^{a+1/2}\int_{-\infty}^{\infty}F(\eta)d\eta. \tag{19}$$

Therefore, we have $a=-1/2$, and the deficit of wake velocity on the centerline is decreasing as $x^{-1/2}$, which is again consistent with experimental data [6]. Inserting this value into Eq. (18) and integrating twice gives Goldstein's [8] solution

$$F(\eta)=Ce^{-\eta^2/4}, \tag{20}$$

satisfying zero value and derivative as $\eta\to\pm\infty$ and zero slope at $\eta=0$. The integral constraint (19) then determines the constant $C=D/2\sqrt{\pi}$. For w and $\alpha(x)$, we posit the compatible similarity forms

$$w(x,y)=Cx^{-1/2}f(\eta),\quad \alpha(x)=\alpha_0x^{1/2}.$$

Then Eq. (16b) provides the equation for $f(\eta)$, namely,

$$f''-\lambda^2f=e^{-\eta^2/4}, \tag{21}$$

where $\lambda^2=1/\alpha_0^2$. This has the even homogeneous solution

$$f_e(\eta)=A\cosh\lambda\eta$$

and the particular solution

$$f_p(\eta)=\frac{\lambda\sqrt{\pi}}{2}e^{\lambda^2}\left[e^{\lambda\eta}\,\mathrm{erf}\left(\frac{\eta+2\lambda}{2}\right)-e^{-\lambda\eta}\,\mathrm{erf}\left(\frac{\eta-2\lambda}{2}\right)\right]. \tag{22}$$

Satisfaction of $f(\pm\infty)\to0$ on the general solution $f=f_e+f_p$ gives

$$A=\sqrt{\pi}\lambda e^{\lambda^2}.$$

Thus, the exact solution to the Prandtl α equations for the mean deficit velocity in a classical turbulent wake is

$$f(\eta)=\sqrt{\pi}\lambda e^{\lambda^2}\left[\cosh\lambda\eta-\left\{\frac{e^{\lambda\eta}}{2}\,\mathrm{erf}\left(\frac{\eta+2\lambda}{2}\right)-\frac{e^{-\lambda\eta}}{2}\,\mathrm{erf}\left(\frac{\eta-2\lambda}{2}\right)\right\}\right]. \tag{23}$$

A least-squares fit to the most recent and complete data of Wygnanski *et al.* [9] yields $\lambda=3.059$. These results are compared in Fig. 1 which also displays the earlier data of Townsend [10] and the standard prediction $f(\eta)=e^{-0.693\eta^2}$ from mixing-length theory [6]. The pesent theoretical result is close to that of mixing-length theory: however, while our prediction (23) does a slightly better job describing the tails of both experimental datasets, mixing-length theory gives a slightly better fit to the inner portion of the measurement of Wygnanski *et al.*

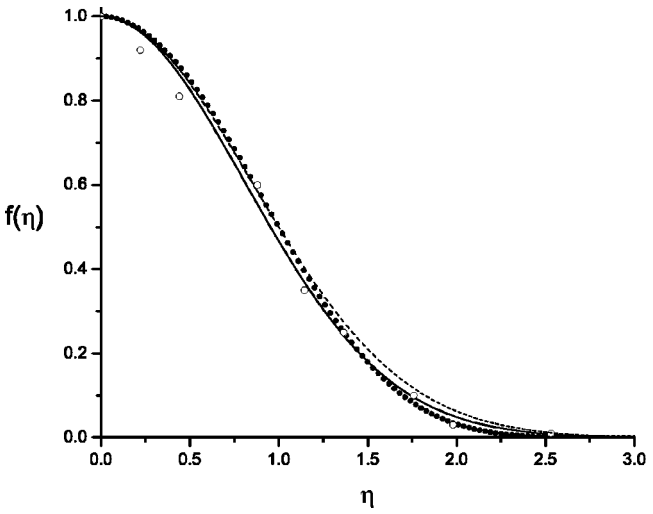

FIG. 1. Least-squares fit (solid line) of Eq. (23) to the recent measurements of Wygnanski *et al.* [9], for which $\lambda=3.059$. Both the data of Wygnanski *et al.* (full circles) and the data of Townsend [10] (open circles) are displayed. Also shown is the standard mixing-length theory result (dashed line) reported in Ref. [6].

The numerical value of Λ can be extrapolated using experimental data for growth of the wake's thickness. Let us denote $\delta(x)$ the transverse distance from the symmetry plane, where velocity deficit achieves the value of half of the maximum velocity deficit in the center. Since we know from experiment that $\delta(x)$ grows proportionally to $\sqrt{x}$, we can deduce the width of the wake in the dimensional coordinates from the experiment as $\delta(x)=\sqrt{l_ex}$, where l_e has the dimension of length. Our theoretical prediction gives $\delta(x)=\eta_{1/2}\sqrt{\Lambda x/U_\infty}$, where U_∞ is the velocity of undisturbed flow far away from the wake, and $\eta_{1/2}$ is defined by $f(\eta_{1/2})=1/2$. From Fig. 1, we observe that $\eta_{1/2}\simeq1$, so $\Lambda=l_eU_\infty$, and the ratio of Λ to the kinematic viscosity ν is just l_eU_∞/ν, i.e., the Reynolds number based on the length scale l_e. This allows for a numerical estimate of the ratio Λ/ν. For example, Townsend's data [10] yield $l_e\simeq0.0015$ cm, velocity of the air flow $U_\infty=1120$ cm/sec. Since the kinematic viscosity of air is $\nu\simeq0.15$ cm^2/sec, we conclude that $\Lambda/\nu\simeq9$.

B. The dragless wake

For self-propelled bodies $D=0$, and consequently Eq. (19) no longer provides a condition for determining the scaling exponent a. Another conservation law must be derived for the case of a dragless wake. In pursuit of this, Eq. (17) is multiplied by y^2 and integrated across the wake to obtain

$$\int_{-\infty}^{\infty} y^2 w_{1x}\, dy = \int_{-\infty}^{\infty} w_{1yy}\, dy.$$

Two integrations by parts, using the zero velocity and slope far-field boundary conditions, give

$$J_2 = \int_{-\infty}^{\infty} y^2 w_1\, dy, \tag{24}$$

showing that the second moment of deficit velocity is conserved. This integral invariant for momentumless laminar planar wakes is known [11].

Inserting the similarity solution form

$$w_1(x,y) = x^a F(\eta), \quad \eta = \frac{y}{\sqrt{4x}} \tag{25}$$

into integral constraint (24) yields

$$J_2 = 8\, x^{a+3/2} \int_{-\infty}^{\infty} \eta^2 F(\eta)\, d\eta. \tag{26}$$

Therefore, the conservation of the second moment is possible if $a = -3/2$. Thus, the velocity deficit on the center line of a two-dimensional (2D) momentumless wake attenuates as $x^{-3/2}$, which is considerably more rapid than the $x^{-1/2}$ decay of the classical wake. As before, we take $\alpha(x) = \alpha_0 x^{1/2}$. The complete solution of this problem is given in the Appendix, Sec. 1. The velocity deficit is $w(x,y) = x^{-3/2} f(\eta)$, where

$$f(\eta) = \frac{e^{\lambda^2/4}}{4}\left[2\cosh\lambda\eta - \frac{4}{\sqrt{\pi}\lambda} e^{-\eta^2 - \lambda^2/4} - e^{\lambda\eta}\,\mathrm{erf}\left(\frac{\lambda}{2} + \eta\right) - e^{-\lambda\eta}\,\mathrm{erf}\left(\frac{\lambda}{2} - \eta\right)\right], \tag{27}$$

in which $\lambda = 2/\alpha_0$.

The velocity deficit profile computed from Eq. (27) is the curve labeled 2D in Fig. 2. We have not been able to locate experimental data for planar dragless wakes with which to compare our theoretical results.

V. AXISYMMETRIC WAKES

Here the flow of streamwise velocity $U_\infty = 1$ aligned with the axis of a body of revolution giving rise to an axisymmetric wake is considered. The analysis follows closely that for the axisymmetric classical and dragless wakes in Sec. III, so we simply outline the results in a cogent fashion. It may be observed that a derivation of the governing equations for axisymmetric boundary-layer flow follows closely that for planar flow. The fundamental difference lies in the leading order diffusion operators that appear in Eqs. (14a) and (14c): whereas in the planar case, the diffusion operator is $\partial^2/\partial y^2$, in the axisymmetric case it is $\partial^2/\partial r^2 + 1/r\,\partial/\partial r$, where (r,z) are cylindrical coordinates. The incompressibility condition (14b) is changed to

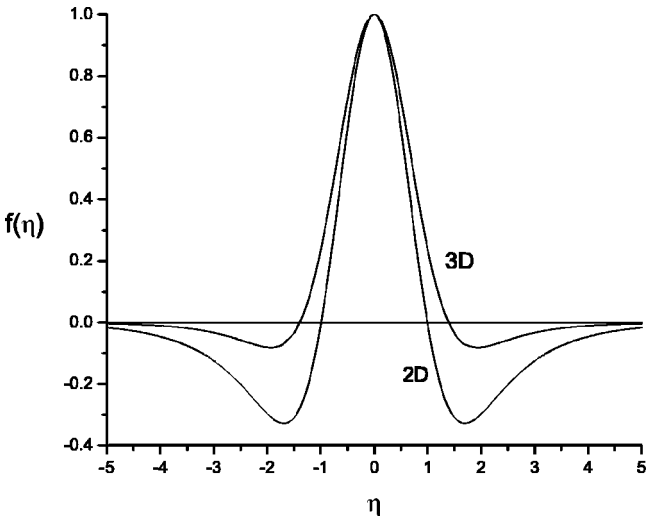

FIG. 2. Self-similar mean turbulent streamwise velocity deficit profiles for both planar (2D) and axisymmetric (3D) dragless wakes.

$$\frac{\partial U_r}{\partial r} + \frac{U_r}{r} + \frac{\partial U_z}{\partial z} = 0.$$

A. The classical wake

For an axisymmetric wake behind a body of drag D, the momentum deficit carried by the wake is given by

$$D = 2\pi \int_0^{\infty} r w_1(z,r)\, dr, \tag{28}$$

where (r,z) are cylindrical polar coordinates. Assume a self-similar deficit velocity of the form $w_1 = z^a F(\eta)$ with $\eta \sim r z^{-b}$. The axisymmetric analogs of Eqs. (17) and (16b) are

$$\frac{\partial w_1}{\partial z} = \frac{\partial^2 w_1}{\partial r^2} + \frac{1}{r}\frac{\partial w_1}{\partial r}, \tag{29a}$$

$$w_1 = w - \alpha^2\left(\frac{\partial^2 w}{\partial r^2} + \frac{1}{r}\frac{\partial w}{\partial r}\right). \tag{29b}$$

Inserting the similarity solution forms into Eq. (29a) gives $b = 1/2$ and from Eq. (28) it follows that $a = -1$. Thus, the width of the wake is growing proportional to $z^{1/2}$ and center line velocity deficit decreases as z^{-1}, which is again consistent with experiments [6].

For the choice $\alpha(z) = \alpha_0 z^{1/2}$, the solution for the wake velocity deficit function $f(\eta)$ is derived in the Appendix, Sec. 2. The result is

$$f(\eta) = \frac{D}{\pi}\left[I_0(\lambda\eta)\left(C_1(\lambda^2/4) - \int_0^{\eta} \lambda^2 t K_0(\lambda t) e^{-t^2}\, dt\right) + K_0(\lambda\eta)\int_0^{\eta} \lambda^2 t I_0(\lambda t) e^{-t^2}\, dt\right], \tag{30}$$

where

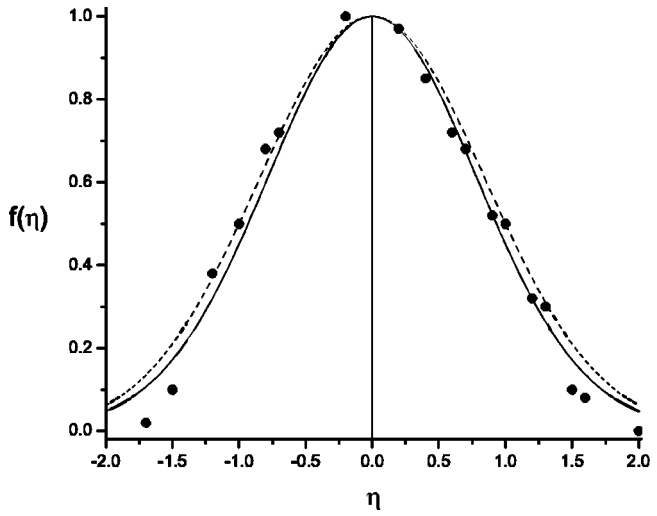

FIG. 3. Least-squares fit ($\lambda = 3.35$) of the axisymmetric wake velocity deficit profile given in Eq. (30) (solid line) to the experimental data (solid circles) of Uberoy and Freymuth [12]. The standard mixing-length theory prediction [6] is also shown (dashed line) for comparison.

$$C_1(s) = -se^s \mathrm{Ei}(-s).$$

Here, D is the drag on the body, $\lambda = 2/\alpha_0$, and $\mathrm{Ei}(z) = -PV\int_{-z}^{\infty}(e^{-t}/t)dt$ is the exponential integral. A least-squares fit of Eq. (30) to the experimental results of Uberoy and Freymuth [12] yields $\lambda = 3.35$ and this comparison between theory and experiment is displayed in Fig. 3. Also included is the prediction $f(\eta) = e^{-\ln(2)\eta^2}$ from mixing-length theory [6].

B. The dragless wake

For the axisymmetric dragless wake, the net wake momentum is zero so Eq. (28) does not apply. In this case, the integral constraint is found by multiplying the governing equation (29a) by r^3 and integrating across the wake to obtain

$$J_3 = \int_0^{\infty} r^3 w_1 \, dr, \tag{31}$$

showing that the third moment of the wake deficit velocity is conserved [11]. Now insert the ansatz $w_1 = z^a F(\eta)$ and $\eta \sim r z^{-b}$ into Eqs. (29a) and (31) to find similarity exponents $b = 1/2$ and $a = -2$. The relevant solution for $F(\eta)$ is now $F(\eta) = C(\eta^2 - 1)e^{-\eta^2}$, where, from Eq. (31), we find $C = J_3/\pi$. Now for $w = Cz^{-3/2} f(\eta)$ and using the convenient choice $\eta = r/\sqrt{4z}$, Eq. (29b) gives

$$f'' + \frac{1}{\eta} f' - \lambda^2 f = -(\eta^2 - 1)e^{-\eta^2}. \tag{32}$$

As in the preceding section, $\alpha(z) = \alpha_0 z^{1/2}$. The solution for the axisymmetric dragless wake is, to within a constant multiplier,

$$f(\eta) = I_0(\lambda\eta)\left[C_1(\lambda^2/4) - \lambda^2 \int_0^{\eta} tK_0(\lambda t)e^{-t^2} dt\right] + K_0(\lambda\eta)\lambda^2 \int_0^{\eta} t(t^2 - 1)I_0(\lambda t)e^{-t^2} dt, \tag{33}$$

where $\lambda = 2/\alpha_0$ and

$$C_1(s) = 4s \int_0^{\infty} t(t^2 - 1)K_0(\lambda x)e^{-t^2} dt = -s + s^2 e^s \mathrm{Ei}(-s).$$

Solution (33) is the curve labeled 3D in Fig. 2. Unfortunately, experimental data for the dragless wake [13] were taken too close to the body for the self-similar regime to have developed, so we cannot compare those results with our asymptotic solution.

VI. DISCUSSION AND CONCLUSION

We have derived a modified form of Navier-Stokes α model for the case when α is spatially dependent. It is argued that the coefficient of the dissipation term does not have to be equal to the kinematic viscosity as previous works have suggested. We have also derived the corrected form of Prandtl α equations which now yield conservation of streamwise momentum. Based on these equations, four different analytical solutions describing turbulent wakes using the Navier-Stokes α model of mean turbulent flow have been found. The predictions of the model agree well with available experiments for classical wakes, though the difference between mixing-length theory and the present results for the planar wake may be considered insignificant. Our method also paves the way for an explicit estimation of the dissipation coefficient from experimental data. The strength of Navier-Stokes α model lies in the fact that self-similar solutions and exponents agreeing with experimental data appear automatically without the need of extra assumptions. The testing of Navier-Stokes α equations in the boundary-layer limit has the extra advantage that any ambiguity in the choice of the dissipation coefficient Λ is removed by the scaling. The result is that only a one-parameter fit to experimental data is required.

The variable $\alpha(x)$ was chosen to be proportional to the width of the boundary layer to assure self-similarity. This is the only physically feasible choice since α is the rms of Lagrangian fluctuations of the particle position. In a turbulent boundary layer, fluid particles can move across the boundary layer, so the fluctuation amplitude at a given point is approximately equal to thickness of boundary layer at this point, and the rms of fluctuations are thus of the order of boundary-layer thickness as well.

The two features of Navier-Stokes α model ($\Lambda \gg \nu$ and α being of the same order as boundary-layer thickness) clearly invoke analogy with the standard mixing-length theory of turbulence. Numerically, these two completely different approaches yield similar results. Since the derivation of the Euler α equation is rigorous, the main weakness of the Navier Stokes α model lies in complete lack of theory for the

dissipation term, and a rigorous derivation of this term would be of paramount importance.

ACKNOWLEDGMENTS

We acknowledge illuminating discussions with D. Holm and B. Wingate on the subject of this paper. In particular, Eq. (9) was derived by D. Holm, B. Wingate, and the authors. The hospitality of CNLS and TWG at Los Alamos National Laboratory, where V.P. was spending one day a week, is gratefully acknowledged. V.P. was partially supported by a SURP grant.

APPENDIX: SOME DETAILS OF SOLUTIONS

1. Dragless wakes in two dimensions

Inserting Eq. (25) into Eq. (17) gives the boundary-value problem

$$F''+2\eta F'+6F=0; \quad F'(0)=0, \quad F(\infty)=0,$$

with solution

$$F(\eta)=Ce^{-\eta^2}H_2(\eta), \tag{A1}$$

where the second Hermite polynomial is $H_2(\eta)=4\eta^2-2$. The constant C determined from Eq. (24) is $C=J_2/16\sqrt{\pi}$. Compatible forms for $w(x,y)$ and $\alpha(x)$ are

$$w(x,y)=Cx^{-3/2}f(\eta), \quad \alpha(x)=\alpha_0 x^{1/2},$$

which, when inserted into Eq. (16b), yields

$$f''-\lambda^2 f=(4\eta^2-2)e^{-\eta^2}, \tag{A2}$$

where $\lambda^2=4/\alpha_0^2$. The solution of Eq. (A2) satisfying the vanishing boundary conditions at infinity is Eq. (27).

2. Axisymmetric wakes with drag

A convenient choice for the similarity variable is $\eta=2r/\sqrt{z}$ and inserting $w_1=z^{-1}F(\eta)$ into Eq. (29a) yields the boundary-value problem

$$F''+\frac{1}{\eta}F'=-4F-2\eta F'; \quad F'(0)=0, \quad F(\infty)=0,$$

with solution $F(\eta)=Ce^{-\eta^2}$. From Eq. (28), one obtains $C=D/\pi$. The equation for w is determined from Eq. (29b). Inserting w_1 and $w=Cz^{-1}f(\eta)$ in Eq. (29b) with the choice $\alpha^2=\alpha_0^2 z$, $\lambda^2=4/\alpha_0^2$ yields

$$f''+\frac{1}{\eta}f'-\lambda^2 f=e^{-\eta^2}. \tag{A3}$$

The homogenous solutions are $I_0(\lambda\eta)$ and $K_0(\lambda\eta)$. A particular solution $f_p(\eta)$ obtained by variation of parameters is

$$f_p(\eta)=-I_0(\lambda\eta)\lambda^2\int_0^\eta tK_0(\lambda t)e^{-t^2}dt + K_0(\lambda\eta)\lambda^2\int_0^\eta tI_0(\lambda t)e^{-t^2}dt. \tag{A4}$$

Thus, the general solution is $f(\eta)=C_1I_0(\lambda\eta)+C_2K_0(\lambda\eta)+f_p(\eta)$, where C_1 and C_2 are determined from boundary conditions. Although $K_0(\lambda\eta)$ in Eq. (A4) is singular as $\eta\to 0$, the integral multiplying it is of order η^2 so the entire term remains regular. Therefore, the singular $C_2K_0(\lambda\eta)$ component of the homogeneous solution is necessarily zero, i.e., $C_2=0$.

In the limit $\eta\to\infty$, the term multiplying $I_0(\lambda\eta)$ in Eq. (A4) becomes

$$\lambda^2\int_0^\infty tK_0(\lambda t)e^{-t^2}dt=-se^s\mathrm{Ei}(-s)\equiv C_1(s), \tag{A5}$$

where $s=\lambda^2/4$. This leads to the formula (30).

[1] S. Chen, C. Foias, D.D. Holm, E. Olson, E.S. Titi, and S. Wynne, Phys. Rev. Lett. **81**, 5338 (1998); Phys. Fluids **11**, 2343 (1999); Physica D **133**, 49 (1999).

[2] C. Foias, D.D. Holm, and E.S. Titi, Physica D **152-153**, 505 (2001); Dyn. Diff. Eqns. **14**, 1 (2002).

[3] J.E. Marsden and S. Shkoller, Proc. R. Soc. **359**, 1449 (2001).

[4] A. Cheskidov, C. R. Acad. Sci., Ser. I: Math. **334**, 1 (2002).

[5] D.D. Holm, Physica D (to be published).

[6] H. Schlichting, *Boundary Layer Theory*, 7th ed. (McGraw-Hill, New York, 2000).

[7] D.D. Holm, V. Putkaradze, B. Wingate, and P.D. Weidman (unpublished).

[8] S. Goldstein, Cambridge Philos. Soc. **26**, 30 (1930).

[9] I. Wygnanski, F. Champagne, and B. Marasli, J. Fluid Mech. **168**, 31 (1986).

[10] A. Townsend, Proc. R. Soc. London, Ser. A **197**, 124 (1949).

[11] B. Birkhoff and E.H. Zarantonello, *Jets, Wakes and Cavities* (Academic Press, New York, 1957), pp. 307 and 308.

[12] M.S. Uberoy and P. Freymuth, Phys. Fluids **13**, 2205 (1970).

[13] J.A. Schetz and A.K. Jakubowski, AIAA J. **13**, 1568 (1975).